Limits of Smart Radio Resource Assignment in GEO Satellite Communications

Tedros Salih Abdu, Steven Kisseleff, Eva Lagunas and Symeon Chatzinotas
Interdisciplinary Centre for Security, Reliability and Trust (SnT),
University of Luxembourg, Luxembourg
Email: {tedros-salih.abdu, steven.kisseleff, eva.lagunas, symeon.chatzinotas}@uni.lu

***Abstract*—In this paper, the limits in terms of offered capacity for a non-precoded geostationary (GEO) satellite communication system is investigated. In particular, we focus on the smart radio resource assignment as a technique to manage the interference across the multi-beam pattern of the GEO system. In this context, a joint power and carrier allocation problem is formulated to maximize the capacity of the system. The formulated optimization problem is non-convex and difficult to solve. Hence, we propose to address the frequency allocation first by assuming an equal power distribution, followed by the optimal power assignment to maximize the sum-capacity. Numerical evaluations are presented comparing the proposed method with a precoded-based system and with benchmark resource allocation schemes, showing the benefits of the proposed technique and identifying the limits of a non-precoded GEO satellite communications system.**

***Index Terms*—GEO satellite, Radio Resource Assignment, Sum-Capacity Maximization**

I. Introduction

Satellite communication systems have the capability of providing a handful of services, from TV broadcasting to broadband internet, anywhere in the world at speeds of several megabits per second. As the world undergoes a digital transformation, satellite communications are expected to have a significant role in bridging the digital divide by providing connectivity to remote areas in a quickly and easily manner [1].

The use of multi-spot beams have been introduced in modern satellite communication systems to improve the spectrum utilization. While initial multibeam satellite systems considered uniform and fixed power and bandwidth assignment, the recent advances in on-board payload technology (e.g. digital payloads) allow for an adaptive smart radio resource assignment, where power and bandwidth can be distributed unevenly across beams depending on the channel quality and/or expected beam demand [2], [3].

Several resource optimization techniques have been proposed in the multibeam GEO satellite literature focusing on the beam demand satisfaction. Demand-matching based bandwidth allocation has been proposed in [2] with the objective of minimizing the difference between the requested demand and the offered capacity. In [4] power allocation is optimized to maximize the energy efficiency of the system by neglecting inter-beam interference. The latter is considered in [5], [6]. Joint power and frequency allocation under a demand-matching perspective has been investigated in [7]–[9]. Regarding the maximization of the sum-capacity, several works have focused on the precoding design (including power allocation) assuming full frequency reuse across beams [10], [11].

In this paper, we aim to investigate the limits of a non-precoded satellite system by means of proposing a joint power and carrier assignment approach to maximize the sum-capacity of the system. Although the maximization of system capacity has been extensively studied in terrestrial wireless communications (e.g. [12]–[17]), this has not been fully addressed in the satellite communication area, where different system model and payload constraints apply. In addition, the goal of this paper is to shed some light into the need of complex interference mitigation techniques when flexible and smart resource assignment is available. The contribution the paper described as follows:

- We mathematically formulate the joint carrier and power optimization problem for the system capacity maximization. The problem is shown to be non-convex and NP-hard. Therefore, we propose to solve the problem by splitting it into two sub-problems which are sequentially addressed. The achieved solution is a sub-optimal point of the original problem.
- We provide extensive numerical results, where the performance of the proposed scheme is compared with different non-precoded radio resource management benchmark schemes. In addition, we compared with the popular precoded-based full-frequency reuse strategy [10], [18] and identified when precoding is needed to further increase the system capacity.

The remainder of the paper is organized as follows. Section II introduces the system model. The problem formulation and the proposed solution are presented in Section III and Section

This work has been supported by the Luxembourg National Research Fund (FNR) under the project FlexSAT (C19/IS/13696663), DISBuS and the AFR Grant INSAT - "Power and Bandwidth Allocation for INterference-Limited SATellite Communication Systems".

IV, respectively. Numerical results are provided in Section V. Section VI concludes the paper.

Notation: Boldface of upper case and lower case letters refers to matrices and vectors, respectively. The transpose of a vector and hermitian transpose of a vector are represented by $[.]^T$ and $[.]^H$, respectively. Lastly, $\|.\|_F$ represents the Frobenius norm.

II. System Model

We consider a downlink multibeam GEO satellite system which consists of N beams and K carriers. The total available downlink bandwidth is equal to $B_{tot} = K \cdot B_{sc}$ where each carrier has bandwidth B_{sc}. We assume that a single user per beam is served at a given time instance. Furthermore, we denote $\mathbf{x}_k = \big[x_k[1], x_k[2], \ldots, x_k[N]\big]^T$ the assignment vector for carrier k, where $x_k[i] \in \{0, 1\}$ is a binary valued variable, with $x_k[i] = 1$ indicating that carrier k is assigned to user i. The channel power gain vector between the satellite and the ith user over the kth carrier is denoted as $\mathbf{g}_{i,k} = \big[g_{i,k}[1], g_{i,k}[2], \ldots, g_{i,k}[N]\big]^T$.

The transmit power allocation vector for kth carrier is denoted as $\mathbf{p}_k = \big[p_k[1], p_k[2], \ldots, p_k[N]\big]^T$. Hence, the signal-to-interference-plus-noise ratio (SINR) of the ith user over kth carrier can we expressed as

$$\gamma_{i,k}(\mathbf{x}_k, \mathbf{p}_k) = \frac{g_{i,k}[i]x_k[i]p_k[i]}{\sum_{j=1, j\neq i}^{N} g_{i,k}[j]x_k[i]p_k[j] + \sigma_k^2[i]}, \quad (1)$$

where $p_k[i]$ is the transmit power assigned to the ith user over the kth carrier, $\sigma_k^2[i]$ is the noise power received by the ith user over the kth carrier and $g_{i,k}[j]$ is the channel power gain between the jth satellite antenna and the ith user over the kth carrier. The power channel gain $g_{i,k}[j]$ is defined as

$$g_{i,k}[j] = \left| \frac{\sqrt{G_R G_i[j]}}{4\pi \frac{d_i}{\lambda}} \right|^2, \quad (2)$$

where G_R is the user terminal antenna gain, $G_i[j]$ denotes the gain from the jth satellite feed towards the ith user and d_i is the slant range between the satellite and ith user.

The offered capacity at to user i over carrier k is given by

$$C_{i,k} = B_{sc} \log_2(1 + \gamma_{i,k}(\mathbf{x}_k, \mathbf{p}_k)), \quad (3)$$

and the overall offered capacity at beam i considering the aggregation of all available carriers of the system is

$$C_i = \sum_{k=1}^{K} C_{i,k}. \quad (4)$$

III. Problem Formulation

In this section, the resource allocation problem is formulated to maximize the total capacity of the system. For this, we select the sum of the offered capacity as an objective function subject to different power and carrier constraints. Furthermore, we include a minimum SINR constraint for each user, which prevents that only users with good channel conditions are served while users with weak channels starve. The latter is also achieved by ensuring that at least one carrier is allocated per user. The optimization problem is given by

$$\begin{aligned}
&\underset{\mathbf{x}_k, \mathbf{p}_k, \forall_k}{\texttt{maximize}} \quad f\left(\gamma_{i,k}(\mathbf{x}_k, \mathbf{p}_k)\right) \\
&\texttt{s.t.} \\
&\qquad T1: \gamma_{i,k}(\mathbf{x}_k, \mathbf{p}_k) \geq x_k[i]\gamma_{min}, \forall_i, \forall_k, \\
&\qquad T2: \sum_{i=1}^{N}\sum_{k=1}^{K} p_k[i] \leq P_{total}, \\
&\qquad T3: \sum_{k=1}^{K} p_k[i] \leq P_{max}, \forall_i, \\
&\qquad T4: x_k[i] \in \{0, 1\}, \forall_i, \forall_k, \\
&\qquad T5: \sum_{k=1}^{K} x_k[i] \geq 1, \forall_i, \\
&\qquad T6: p_k[i] \leq x_k[i]P_{max}, \forall_i, \forall_k, \\
&\qquad T7: p_k[i] \geq 0, \forall_i, \forall_k,
\end{aligned} \quad (5)$$

where

$$f\left(\gamma_{i,k}(\mathbf{x}_k, \mathbf{p}_k)\right) = \sum_{i=1}^{N}\sum_{k=1}^{K} B_{sc} \log_2(1 + \gamma_{i,k}(\mathbf{x}_k, \mathbf{p}_k)).$$

Targeting the maximization of total offered capacity in (5), constraint $T1$ ensures that the SINR per carrier is not lower than to the minimum SINR γ_{min} requirement of the system. Constraint $T2$ provides the upper bound for the transmit power given by the total available power at the satellite P_{total}. In addition, $T3$ indicates the per-beam power constraint, where each beam should not exceed the limit imposed by P_{max}.. The carrier assignment $x_k[i]$ is a binary variable as indicated by $T4$. Furthermore, in order to serve all areas in the field of view of the satellite, each beam has to be assigned at least one carrier, which is guaranteed by constraint $T5$. Constraint $T6$ guarantees that the power is allocated to beam i in carrier k only if the carrier is assigned, i.e. $x_k[i] = 1$. Finally, Constraint $T7$ ensures that the allocated power is non-negative. At first, we rewrite problem (5) in standard form of convex optimization:

$$\begin{aligned}
&\underset{\mathbf{x}_k, \mathbf{p}_k, \forall_k}{\texttt{minimize}} \quad -f\left(\gamma_{i,k}(\mathbf{x}_k, \mathbf{p}_k)\right) \\
&\texttt{s.t.} \\
&\qquad T1, T2, T3, T4, T5, T6, T7,
\end{aligned} \quad (6)$$

The non-linearity of $\gamma_{i,k}(\mathbf{x}_k, \mathbf{p}_k)$ as well as the integer nature of $x_{i,k}$ makes the problem (6) to be non-convex. Problem (6) is a mixed integer non-convex optimization problem, for which it is difficult to find the optimal solution. In this section, we propose a sub-optimal solution for the aforementioned problem (6).

IV. Proposed smart radio resource assignment

We solve the problem by splitting it into two subproblems. In the first step, we propose an optimization problem to

find the carrier allocation vector $\mathbf{x}_k$ by assuming a fixed and uniformly distributed power. Next, in the second step and based on the previously obtained carrier assignment, we optimize the power to maximize the system capacity.

A. Step 1: Carrier Assignment

In this section, we solve the carrier allocation problem while keeping the transmit power constant. We assume equal power per carrier i.e. $p_k[i] = \frac{P_{total}}{NK}$. The optimization problem formulated as

$$\begin{aligned} \underset{\mathbf{x}_k,\forall_k}{\texttt{minimize}} \quad & -f\left(\gamma_{i,k}(\mathbf{x}_k)\right) \\ \texttt{s.t.} \quad & \\ & R1: x_k[i] \in \{0,1\}, \forall_i, \forall_k, \\ & R2: \sum_{k=1}^{K} x_k[i] \geq 1, \forall_i, \end{aligned} \tag{7}$$

Constraints $R1$ and $R2$ represent the binary valued variables and the guarantee that at least one carrier per beam is assigned, respectively. We convexify the constraint set of (7) by relaxing $R1$ constraint to be continuous between 0 and 1, i.e. $0 \leq x_k[i] \leq 1$. Since $R1$ is relaxed, we observe that the value of $x_k[i] = 1/K$ also a feasible solution which satisfies the constraint $R2$. Hence, for this case, it is difficult to assign at least one carrier per beam. Therefore, to avoid this problem, we replace $R2$ by equivalent representation of $x_k[i] \geq \chi_k[i], \forall_i, \forall_k$, where $\chi_k[i]$ is the binary carrier allocation when K color reuse pattern is used[1]. Due to the inter-beam interference, the object of (7) is non-linear and non-convex. Hence, it is very challenging to determine a close-to-optimum solution. Therefore, we propose to use the quadratic transform to solve the problem iteratively [19]. The quadratic transform of $f\left(\gamma_{i,k}(\mathbf{x}_k)\right)$ is given by

$$\widetilde{f}\left(\gamma_{i,k}(\mathbf{x}_k)\right) = \log_2(1 + \widetilde{\gamma}_{i,k}(\mathbf{x}_k)) \tag{8}$$

$$\begin{aligned} \widetilde{\gamma}_{i,k}(\mathbf{x}_k) = 2y_{i,k}\sqrt{g_{i,k}[i]x_k[i]p_k[i]} \\ -y_{i,k}^2\left(\sum_{j=1,j\neq i}^{N} g_{i,k}[j]x_k[i]p_k[j] + \sigma_k^2[i]\right) \end{aligned} \tag{9}$$

$$y_k[i] = \frac{\sqrt{g_{i,k}[i]x_k^l[i]p_k[i]}}{\sum_{j=1,j\neq i}^{N} g_{i,k}[j]x_k^l[i]p_k[j] + \sigma_k^2[i]} \tag{10}$$

where $y_k[i]$ is the quadratic transform variable for each carrier and $x_k^l[i]$ is the previous value of $x_k[i]$. Finally, we rewrite (7) as

[1]The value of $\chi_k[i]$ depends on K. For example if $K = 4$ and $K = 7$ then $\chi_k[i]$ holds the property of four color reuse pattern and seven color reuse pattern, respectively.

$$\begin{aligned} \underset{\mathbf{x}_k,\forall_k}{\texttt{minimize}} \quad & -\widetilde{f}\left(\gamma_{i,k}(\mathbf{x}_k)\right) \\ \texttt{s.t.} \quad & \\ & R1: 0 \leq x_k[i] \leq 1, \forall_i, \forall_k, \\ & R2: x_k[i] \geq \chi_k[i], \forall_k, \forall_i, \end{aligned} \tag{11}$$

The problem (11) is convex and can be efficiently solved with advanced optimization toolboxes like CVX [20]. The proposed algorithm is provided in **Algorithm 1**. First , we test the algorithm for different possible values $x_k^l[i]$ and we observed that a feasible point $x_k^l[i] = 1, \forall_k, \forall_i$ gives best result. Therefore, we start with feasible point $x_k^l[i] = 1, , \forall_k, \forall_i$. Then, the new solution of $x_k[i]$ updates the value of $x_k^l[i]$. Accordingly, the algorithm iteratively updates the value of $y_k[i]$ until convergence. For this paper, the algorithm terminates when the absolute difference between the previous and the current value of $y_k[i]$ undergoes 10^{-4} i.e. $\sum_{i=1}^{N}\sum_{k=1}^{K}\left|y_k[i] - y_k^l[i]\right| \leq 10^{-4}$, where $y_k^l[i]$ is the previous value of $y_k[i]$. Note that the final output of the algorithm $x_k[i]$ may not be an integer number due to the applied relaxation of the variables. Therefore, we round it to the nearest integer number.

Algorithm 1: Carrier allocation

Input: feasible point $x_k^l[i]$;
$y_k[i] \leftarrow 0$;
repeat
  $y_k^l[i] \leftarrow y_k[i]$;
  Update: $y_k[i] = \frac{\sqrt{g_{i,k}[i]x_k^l[i]p_k[i]}}{\sum_{j=1,j\neq i}^{N} g_{i,k}[j]x_k^l[i]p_k[j]+\sigma_k^2[i]}$;
  Solve (11) ;
  $x_k^l[i] \leftarrow x_k[i]$;
until $\sum_{i=1}^{N}\sum_{k=1}^{K}\left|y_k[i] - y_k^l[i]\right| \leq 10^{-4}$;
Output:
$x_k[i], \forall_i, \forall_k$;

B. Step 2: Power Allocation

At this point, we have obtained the carrier assignment vectors for each beam. In this section, we optimize the power required per beam to maximize the system sum rate considering the potential inter-beam interference. Then, we reformulate the optimization problem of (6) as follows,

$$\begin{aligned} \underset{\mathbf{p}_k,\forall_k}{\texttt{minimize}} \quad & -f\left(\gamma_{i,k}(\mathbf{p}_k)\right) \\ \texttt{s.t.} \quad & \\ & T1: \gamma_{i,k}(\mathbf{p}_k) \geq x_k[i]\gamma_{min}, \forall_i, \forall_k, \\ & T2: \sum_{i=1}^{N}\sum_{k=1}^{K} p_k[i] \leq P_{total}, \\ & T3: \sum_{k=1}^{K} p_k[i] \leq P_{max}, \forall_i, \\ & T6: p_k[i] \leq x_k[i]P_{max}, \forall_i, \forall_k, \\ & T7: p_k[i] \geq 0, \forall_i, \forall_k, \end{aligned} \tag{12}$$

Problem (12) is still non-convex because of the non-linearity of $\gamma_{i,k}(\mathbf{p}_k)$. Similar to section IV.A, we employ a quadratic transform of the objective function to solve the problem (12) iteratively [19]. The quadratic transform of $f(\gamma_{i,k}(\mathbf{p}_k))$ is given by

$$\widetilde{f}(\gamma_{i,k}(\mathbf{p}_k)) = \log_2(1+\widetilde{\gamma}_{i,k}(\mathbf{p}_k)) \tag{13}$$

$$\begin{aligned}\widetilde{\gamma}_{i,k}(\mathbf{p}_k) &= 2z_{i,k}\sqrt{g_{i,k}[i]p_k[i]} \\ &\quad -z_{i,k}^2\left(\sum_{j=1,j\neq i}^{N} g_{i,k}[j]p_k[j]+\sigma_k^2[i]\right)\end{aligned} \tag{14}$$

$$z_k[i] = \frac{\sqrt{g_{i,k}[i]p_k^l[i]}}{\sum_{j=1,j\neq i}^{N} g_{i,k}[j]p_k^l[j]+\sigma_k^2[i]} \tag{15}$$

where $z_k[i]$ is the quadratic transform variable for each transmit power per carrier and $p_k^l[i]$ is the previous value of $p_k[i]$. Note that we did not include $x_k[i]$ in (13) because we have the constraint $T6$ which guarantees that the power is allocated to beam i in carrier k only if the carrier is assigned, i.e. $x_k[i]=1$. Finally, we rewrite (12) as

$$\begin{aligned}&\underset{\mathbf{p}_k,\forall_k}{\texttt{minimize}} \quad -\widetilde{f}(\gamma_{i,k}(\mathbf{p}_k)) \\ &\texttt{s.t.} \\ &\hat{T}1: x_k[i]\gamma_{min}\left(\sum_{j=1,j\neq i}^{N} g_{i,k}[j]p_k[j]+\sigma_k^2[i]\right) \\ &\qquad -g_{i,k}[i]p_k[i]\leq 0,\forall_i,\forall_k, \\ &T2: \sum_{i=1}^{N}\sum_{k=1}^{K} p_k[i]\leq P_{total}, \\ &T3: \sum_{k=1}^{K} p_k[i]\leq P_{max},\forall_i, \\ &T6: p_k[i]\leq x_k[i]P_{max},\forall_i,\forall_k, \\ &T7: p_k[i]\geq 0,\forall_i,\forall_k,\end{aligned} \tag{16}$$

Note that $\hat{T1}$ is the equivalent form of $T1$. The problem (16) is convex and can be solved optimally. The calculation of the optimal solution for (16) is repeated in each iteration, which is depicted in **Algorithm 2**. First, we start with a feasible point $p_k^l[i]=\frac{p_{total}}{NK}$. Then, we calculate $z_k[i]$ and by solving (16) we obtain a new point $p_k[i]$. The algorithm terminates when the absolute sum of the difference between $z_k[i]$ and $z_k^l[i]$ becomes very small (10^{-4} in this work), which indicates the convergence of the algorithm (being $z_k^l[i]$ the previous value of $z_k[i]$). Correspondingly, the power is optimized such that maximum capacity of the system attained. Accordingly, we obtain the total capacity as $C=\sum_{i=1}^{N}\sum_{k=1}^{K} C_{i,k},\forall_i$.

Algorithm 2: Power allocation

Input: feasible point $p_k^l[i]$;
$z_k[i]\leftarrow 0$;
repeat
  $z_k^l[i]\leftarrow z_k[i]$;
  Update: $z_k[i]=\frac{\sqrt{g_{i,k}[i]x_k[i]p_k^l[i]}}{\sum_{j=1,j\neq i}^{N} g_{i,k}[j]x_k[i]p_k^l[j]+\sigma_k^2[i]}$;
  Solve (16) ;
  $p_k^l[i]\leftarrow p_k[i]$;
until $\sum_{i=1}^{N}\sum_{k=1}^{K}\left|z_k[i]-z_k^l[i]\right|\leq 10^{-4}$;
Output:
$C=\sum_{i=1}^{N}\sum_{k=1}^{K} C_{i,k},\forall_i$;

V. Simulation Results

In this section, we evaluate the performance of the proposed Joint Power and Carrier Sum Rate Maximization (JPCSRM) scheme. The main simulation parameters are summarized in Table I. A $N=100$ GEO satellite beam pattern generated assuming a Direct Radiating Antenna (DRA), with 750 elements spaced 5 lambda and provided by the European Space Agency (ESA) is considered. The results have been generated with $M=100$ Monte Carlo runs. In each run, a user is selected randomly from the considered beam coverage area.

TABLE I
System Parameters

Parameter	Value
Satellite Orbit	13°E
Number of beams (N)	100
Number of carrier (K)	4
System Bandwidth (B_{tot})	500 MHZ
Sub-carrier bandwidth (B_{SC})	125 MHz
Noise power ($\sigma_k^2[i]$)	-123 dBW
Minimum SINR (γ_{min})	-2.2 dB
Max. beam gain ($G_i[j]$)	51.8 dBi
User antenna gain (G_R)	39.8 dBi
Total Power of the system (P_{total})	5000W
Maximum power for each beam (P_{max})	100W

For comparison, we consider the following benchmark schemes:

1) **Full color reuse scheme with uniform power allocation (FullCUP)**: We assume all carriers are used in all beams, i.e. $x_k[i]=1,\forall_i,\forall_k$, and we apply equal power per carrier.
2) **Four color reuse scheme with uniform power allocation(FourCUP)**: One fourth of the available bandwidth with uniform power allocation to each beam is assigned.
3) **Minimum Mean Squared Error (MMSE) precoder**: Full frequency reuse is assumed and the MMSE precoder is applied. The precoding matrix $\mathbf{W}_k$ is obtained from the channel matrix $\mathbf{H}_k$ as follows,

$$\mathbf{W}_k = \sqrt{\frac{P_{total}}{K}}\frac{\widetilde{\boldsymbol{W}}_k}{\|\widetilde{\boldsymbol{W}}_k\|_F} \tag{17}$$

$$\widetilde{\boldsymbol{W}}_k = \mathbf{H}_k^H(\mathbf{H}_k\mathbf{H}_k^H+\beta\mathbf{I})^{-1} \tag{18}$$

where $\beta > 0$ is the regularizer factor, the channel matrix is $\mathbf{H}_k = \left[\mathbf{h}_{1,k}^T, \mathbf{h}_{2,k}^T, \ldots, \mathbf{h}_{N,k}^T\right]^T$ and the channel vector is $\mathbf{h}_{i,k}^T = \left[h_{i,k}[1], h_{i,k}[2], \ldots, h_{i,k}[N]\right]^T$. Note that $h_{i,k}[j]$ is the channel between the jth satellite antenna and the ith user over the kth carrier. Hence, we define the channel as

$$h_{i,k}[j] = \sqrt{g_{i,k}[j]} e^{-\mathrm{i}\Phi_j}, \tag{19}$$

where Φ_j is the phase of the satellite jth antenna. The SINR for the ith user over the kth carrier after using MMSE precoder is

$$\gamma_{i,k}(\mathbf{w}_{i,k}) = \frac{|\mathbf{h}_{i,k}^H \mathbf{w}_{i,k}|^2}{\sum_{j=1, j\neq i}^{N} |\mathbf{h}_{i,k}^H \mathbf{w}_{j,k}|^2 + \sigma_k^2[i]}. \tag{20}$$

Hence, the overall offered capacity at beam i considering the aggregation of all available carriers of the system is

$$C_i = \sum_{k=1}^{K} B_{sc} \log_2(1 + \gamma_{i,k}(\mathbf{w}_{i,k})). \tag{21}$$

A. Random User Location

For each Monte Carlo realization, we choose the location of users randomly from a uniform distribution within the considered beam coverage. Fig. 1 shows the distribution of possible user locations within a beam. Zone-based user location is proposed in Section V.B.

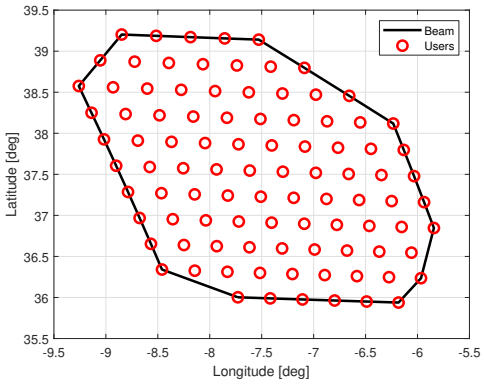

Fig. 1. Location of users within a beam

Fig. 2 shows the CDF of the sum rate for JPCSRM and the benchmark schemes. We observe that the performance JPCSRM outperforms the FullCUP and FourCUP schemes. For example, for 100% cases, JPCSRM achieves 77.66 Gbps while FullCUP and FourCUP achieve 65.56 Gbps and 53.7 Gbps, respectively. However, the achievable rate with JPCSRM is lower than with MMSE precoder by 38.4%. The reason is that the selected user may be located at the beam edge and experience strong interference from the neighboring beams. This interference can be reduced via precoding.

The geographic representation of the average achievable rate per beam for JPCSRM is shown in Fig. 3. We observed that 46% of the beams have a maximum rate between 500 Mbps and 700 Mbps, 26% of the beams have a maximum rate between 700 Mbps and 800 Mbps, 10% of the beams have maximum rate between 800 Mbps and 1000 Mbps, whereas 18% of beams achieves more than 1000 Mbps. In general, we observe that higher rates can be obtained at the border of the coverage area. The reason for this lies in reduced number of interfering beams at the border compared to the center of the coverage area, which leads to lower interference at the border and a higher data rate.

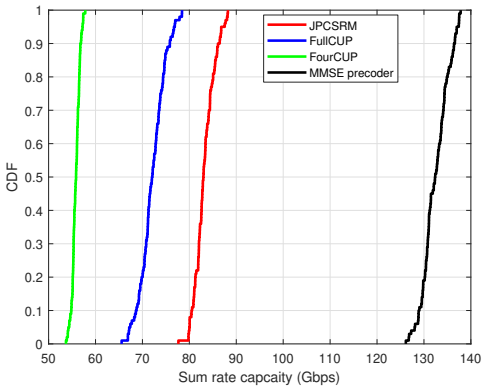

Fig. 2. Comparison of schemes for random user selection

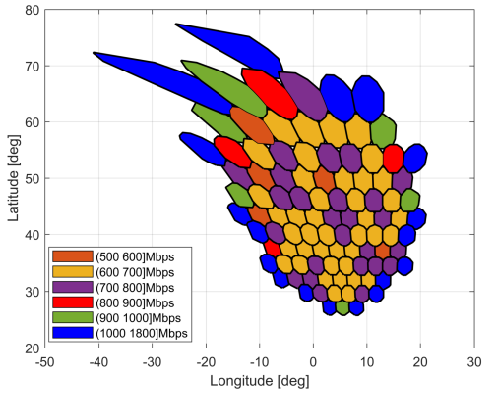

Fig. 3. Average achievable rate per beam for random user location

B. Zone-based User Location

In order to provide a deeper insight in the performance, we subdivide the beam area into two zones, i.e. Zone a and Zone b, see Fig. 4. Zone a contains the users located close to the beam center and Zone b contains the users close to the beam edge. The latter is an important scenario, since users at the beam edge suffer from strong interfering signals of the adjacent beams.

Fig. 5 provides the CDF of sum rate for the JPCSRM and the benchmark schemes over different channel realizations for users in Zone a. We observed that the proposed JPCSRM achieves higher sum rate compared to the FullCUP and FourCUP schemes. For example, for 100% cases, the JPCSRM

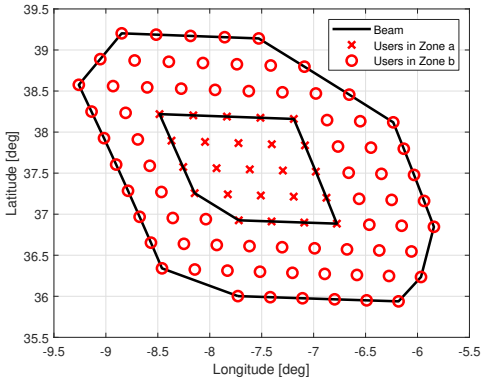

Fig. 4. Users clustered into two zones within a beam

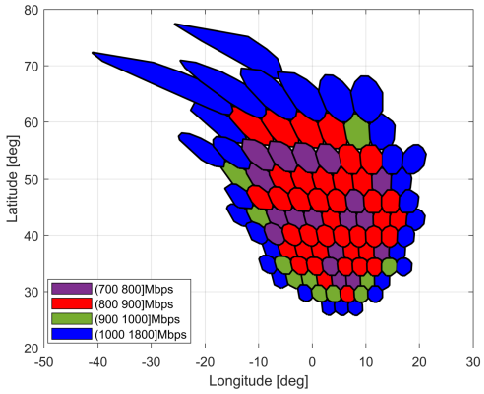

Fig. 6. Average achievable rate per beam Zone a

provides 96.05 Gbps, whereas the sum rate FullCUP and FourCUP scheme is 91.93 Gbps and 62.65 Gbps, respectively. In contrast, the JPCSRM sum rate is lower than with the MMSE precoder by 30%. For Zone a, since the location of the users is near to the center of the beam, we expect the received interference signal from adjacent beams to be rather weak. Hence, we observe a high sum rate.

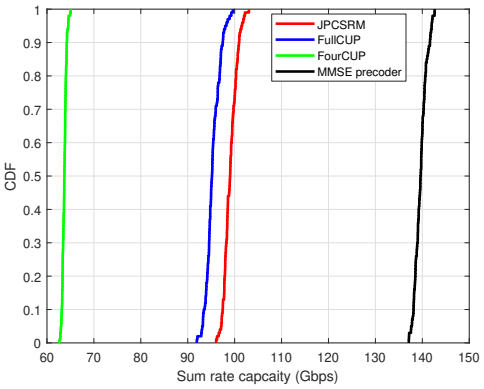

Fig. 5. Comparison of schemes for Zone a

Fig. 6 shows the geographic representation of the average achievable rate per beam. We observed that 18% of the beams have a maximum rate between 700 Mbps and 800 Mbps, 40% of the beams have a maximum rate between 800 Mbps and 900 Mbps, 11% of the beams have a maximum rate between 900 Mbps and 1000 Mbps, whereas 31% of beams provides more than 1000 Mbps. In general, we observe that the sum rate varies much less than in Fig. 6, especially close to the center of the coverage area. The reason is that the users experience much less interference, if they are located close to the beam center. Thus, the data rate depends much less on the number of adjacent interfering beams.

The performance of the schemes for Zone b is shown in Fig. 7. The JPCSRM shows better performance compared to FullCUP and FourCUP. For instance, at 100% cases, the JPCSRM provides 71.95 Gbps whereas, the sum rate of FullCUP and FourCUP is 55.72 Gbps and 50.52 Gbps, respectively. But at 100% cases, the MMSE precoder provides 41.2% more sum rate compared with JPCSRM scheme. This is because the MMSE preocder mitigates the interference while the JPCSRM optimizes the power to minimize the interference. For Zone b, since the location of the users is away from the center of the beam, we expect the received interference signal from adjacent beams to be high. Therefore, we observed that a lower sum rate achieved when the location of the user is near the edge of the beam.

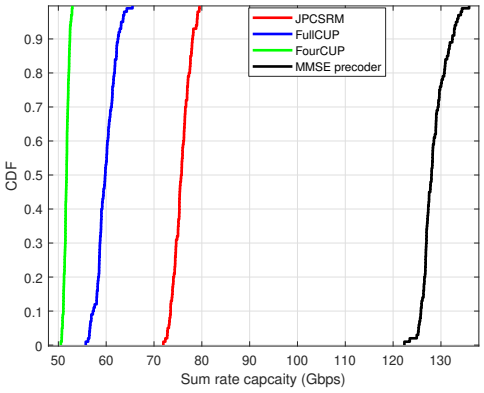

Fig. 7. Comparison of schemes for Zone b

Fig. 8 depicts the geographic representation of the average achievable rate per beam for JPCSRM. We observed that 72% of the beams have a maximum rate between 500 Mbps and 700 Mbps, 4% of the beams have a maximum rate between 700 Mbps and 800 Mbps, 5% of the beams have a maximum rate between 900 Mbps and 1000 Mbps, whereas 19% of beams provides more than 1000 Mbps. We notice that Zone b has a low achievable rate compared to random user distribution and Zone a, because users experience a high level of interference from adjacent beams. Furthermore, high data rates have only been reached at the border of the coverage area, where the number of interfering beam is reduced. From this, we conclude that this scenario is interference-limited and precoding is required in order to enhance the system performance.

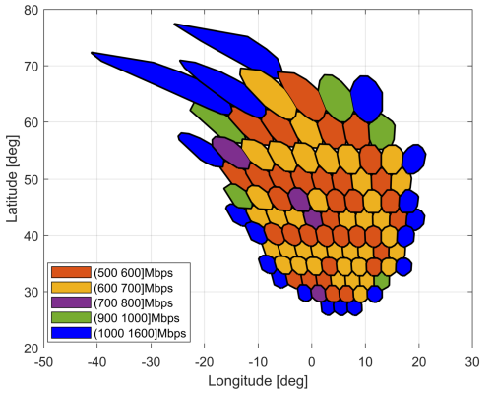

Fig. 8. Average achievable rate per beam Zone b

TABLE II
MAXIMUM SUM RATE AVAILABILITY

		100%	50%	25%	10%
Random Location (Gbps)		77.66	82.98	84.46	86.1
Zone-based Location (Gbps)	Zone a	96.05	99.04	100.1	100.9
	Zone b	71.95	75.66	76.96	78.11

C. Maximum sum rate availability

In this section, we compare the maximum sum rate availability of the different user location distributions for the proposed JPCSRM technique. We can observe from Table II that the system provides 77.66 Gbps, 96.05 Gbps, 71.95 Gbps, in case of random user locations, users in zone a and users in zone b, respectively, in 100% of cases. Similarly, in 50% of cases, the system provides 82.98 Gbps, 99.04 Gbps, 75.66 Gbps, for the same scenarios. Generally, the maximum sum rate of Zone b is lower compared to Zone a and random locations. As described earlier, the reason is much higher interference, which can only be mitigated using precoding

VI. CONCLUSIONS

In this paper, we proposed a joint carrier and power allocation to maximize the capacity of broadband GEO SatCom systems. The formulated optimization problem is non-convex in general and NP-hard. Therefore, we decomposed the original problem into two subproblems. First, we find the carrier assignment assuming a fixed uniform power distribution. Next, we optimize the power required per carrier in order to maximize the capacity of the system. With extensive simulation results, we showed that the achievable capacity of the proposed smart radio resource assignment scheme gives better performance compared to the non-precoded benchmark schemes. Furthermore, we observed that applying proper user selection can push further the limits of the low-complexity smart radio resource assignment. On the other hand, we identify the limits of non-precoded systems by comparing this with high-complexity precoded-based systems.

REFERENCES

[1] O. Kodheli *et al.*, "Satellite Communications in the New Space Era: A Survey and Future Challenges," *IEEE Communications Surveys and Tutorials*, 2020, arXiv:2002.08811.

[2] U. Park, H. W. Kim, D. S. Oh, and B. J. Ku, "Flexible Bandwidth Allocation Scheme Based on Traffic Demands and Channel Conditions for Multi-Beam Satellite Systems," in *IEEE Vehicular Technology Conference*, Sep. 2012, pp. 1–5.

[3] S. Kisseleff, E. Lagunas, T. S. Abdu, S. Chatzinotas, and B. Ottersten, "Radio resource management techniques for multibeam satellite systems," *IEEE Communications Letters*, pp. 1–1, 2020.

[4] T. Qi and Y. Wang, "Energy-efficient power allocation over multibeam satellite downlinks with imperfect CSI," in *2015 International Conference on Wireless Communications Signal Processing (WCSP)*, Oct 2015, pp. 1–5.

[5] C. N. Efrem and A. D. Panagopoulos, "Dynamic Energy-Efficient Power Allocation in Multibeam Satellite Systems," *IEEE Wireless Communications Letters*, vol. 9, no. 2, pp. 228–231, 2020.

[6] A. I. Aravanis, B. Shankar M. R., P. Arapoglou, G. Danoy, P. G. Cottis, and B. Ottersten, "Power Allocation in Multibeam Satellite Systems: A Two-Stage Multi-Objective Optimization," *IEEE Transactions on Wireless Communications*, vol. 14, no. 6, pp. 3171–3182, June 2015.

[7] A. Paris, I. Del Portillo, B. Cameron, and E. Crawley, "A Genetic Algorithm for Joint Power and Bandwidth Allocation in Multibeam Satellite Systems," in *2019 IEEE Aerospace Conference*, March 2019, pp. 1–15.

[8] G. Cocco, T. de Cola, M. Angelone, Z. Katona, and S. Erl, "Radio Resource Management Optimization of Flexible Satellite Payloads for DVB-S2 Systems," *IEEE Transactions on Broadcasting*, vol. 64, no. 2, pp. 266–280, Jun. 2018.

[9] T. S. Abdu, E. Lagunas, S. Kisseleff, and S. Chatzinotas, "Carrier and Power Assignment for Flexible Broadband GEO Satellite Communications System," in *2020 IEEE PIMRC Conference*, August 2020, accepted for presentation.

[10] M. A. Vazquez, A. Perez-Neira, D. Christopoulos, S. Chatzinotas, B. Ottersten, P. Arapoglou, A. Ginesi, and G. Tarocco, "Precoding in multibeam satellite communications: Present and future challenges," *IEEE Wireless Communications*, vol. 23, no. 6, pp. 88–95, 2016.

[11] D. Christopoulos, S. Chatzinotas, and B. Ottersten, "Multicast multigroup precoding and user scheduling for frame-based satellite communications," *IEEE Transactions on Wireless Communications*, vol. 14, no. 9, pp. 4695–4707, Sep. 2015.

[12] Zukang Shen, J. G. Andrews, and B. L. Evans, "Adaptive resource allocation in multiuser ofdm systems with proportional rate constraints," *IEEE Transactions on Wireless Communications*, vol. 4, no. 6, pp. 2726–2737, 2005.

[13] T. Wang and L. Vandendorpe, "Iterative resource allocation for maximizing weighted sum min-rate in downlink cellular ofdma systems," *IEEE Transactions on Signal Processing*, vol. 59, no. 1, pp. 223–234, 2011.

[14] D. T. Ngo, S. Khakurel, and T. Le-Ngoc, "Joint subchannel assignment and power allocation for ofdma femtocell networks," *IEEE Transactions on Wireless Communications*, vol. 13, no. 1, pp. 342–355, 2014.

[15] B. Khamidehi, A. Rahmati, and M. Sabbaghian, "Joint sub-channel assignment and power allocation in heterogeneous networks: An efficient optimization method," *IEEE Communications Letters*, vol. 20, no. 12, pp. 2490–2493, 2016.

[16] Y. Sun, D. W. K. Ng, Z. Ding, and R. Schober, "Optimal Joint Power and Subcarrier Allocation for Full-Duplex Multicarrier Non-Orthogonal Multiple Access Systems," *IEEE Transactions on Communications*, vol. 65, no. 3, pp. 1077–1091, March Mar. 2017.

[17] C. Kai, H. Li, L. Xu, Y. Li, and T. Jiang, "Joint subcarrier assignment with power allocation for sum rate maximization of d2d communications in wireless cellular networks," *IEEE Transactions on Vehicular Technology*, vol. 68, no. 5, pp. 4748–4759, 2019.

[18] V. Joroughi, E. Lagunas, S. Andrenacci, N. Maturo, S. Chatzinotas, J. Grotz, and B. Ottersten, "Deploying joint beam hopping and precoding in multibeam satellite networks with time variant traffic," in *2018 IEEE Global Conference on Signal and Information Processing (GlobalSIP)*, 2018, pp. 1081–1085.

[19] K. Shen and W. Yu, "Fractional programming for communication systems—part i: Power control and beamforming," *IEEE Transactions on Signal Processing*, vol. 66, no. 10, pp. 2616–2630, 2018.

[20] M. Grant and S. Boyd, "CVX: Matlab software for disciplined convex programming, version 2.1," http://cvxr.com/cvx, Mar. 2014.